Indoor Localization based on multi-rate IMU/RSSI Sensor Fusion

Warapon Kumkeaw[*], Veerachai Malyavej[**] and **Manop Aorpimai[**]**

[*] Electrical Engineering Graduate Program, [**] Control, Instrumentation and Mechatronics Engineering
Faculty of Engineering, Mahanakorn University of Technology,
140 Cheum-sampan Rd., Nong Chok, Bangkok, THAILAND
Email: veeracha@mut.ac.th

Manuscript received July 4, 2013
Revised August 19, 2013

ABSTRACT

Localization is the crucial problem for mobile robot navigation. For indoor mobile robot, since a global positioning system (GPS) is incapable, another promising technique to detect the position is the received signal strength indicator (RSSI) from wireless communication. To improve the precision and robustness of mobile unit localization, an inertial measurement unit (IMU) is normally used. In this report, we propose the algorithm for mobile robot localization based on sensor fusion between RSSI from wireless local area network (WLAN) and an IMU. The proposed fusion scheme is based on the extended Kalman filter (EKF). The experiment is conducted by using mobile unit equipped with low-cost IMU and a wireless communication module together with access points to evaluate the performance of our algorithm, and the result is promising.

Keyword: *Robot localization, Kalman filter, RSSI, IMU*

1 INTRODUCTION

Mobile unit localization is the most fundamental and important problem in many applications such as unmanned autonomous vehicles, mobile robots in explore, search and rescue operation, asset tracking in warehouse, etc. Since past few decades, there has been extensive research in this area. Depending on various types of sensor, there are many approaches for localization. In general, however, there are two types of sensor using in localization, namely relative position or inertial sensors and absolute position sensor. We refer the reader to [1], [2] for a survey.

The relative sensor, e.g., an odometer and an IMU or an inertial navigation system (INS), provides the implicit pose's information relative to initial pose. The method to obtain a pose of an object, then, involves in integration, and, hence, suffers from bias that, even a tiny, causes huge error in long run. Certain schemes need to be used to reset an error intermittently. The advantage of this type of sensor is that it relies on its own system not on other references or outside environment that cannot be manipulated.

The absolute sensor provides the information on the distance or orientation relative to known-position references. In theory, it requires multiple references in localization based on these sensors; for example, three distances or angles are necessary to identify a unique position in two-dimensional plane. These methods are also known as trilateration in distance based and triangulation in orientation based. Currently, the most widely used localized method based on relative distance is the GPS, in which distances from at least four references (satellites) are required to identify a unique position of an object in 3-dimensional space. For trilateration, the distance information may inherit from time of flight of the beacon signal from references. Hence, it requires very precise time synchronization between references and a mobile unit, as in, for example, the GPS. Another way to obtain distance is from power loss of the beacon signal from references. This method, as used in this paper, is recently received much attention, since it is relatively low cost due to the vast availability of wireless communication system in both

outdoor and indoor environment. This absolute sensor based method relies on wireless communication link between a mobile unit and remote references, so it normally suffers from the loss of communication or interference from outside environment such as in tunnel or building. The localization method, however, has no drift effect since there is no integration require.

Most of practical navigation system, however, makes use of advantages from both relative and absolute sensors as a complementary to their weakness, for example GPS/IMU/INS sensor fusion, particularly for low cost devices, in which huge amount of research can be found; see refs. [3] - [6]. There are also many localization methods dealing with various types of sensor fusion; for example, in [7], the distance induced from time of flight of data packet from ultra wide band (UWB) communication is used to handle the drifting effect from IMU sensors in pose estimation of human gesture. In [8], [9], the visual sensing and IMU are used in pose estimation of mobile robot. Recently published paper [10] provides comprehensive review of various methods for general sensor fusion—not particular for navigation purpose or certain types of sensor.

Since the GPS system is incapable for indoor environment due to communication disruption, the transmitted power loss form wireless communication link, or RSSI, is, therefore, a promising method to derive distances from known-position references. The localization based on RSSI has been a popular research topic for a few decade due to the widely used of wireless communication in mobile phone as well as WLAN. Furthermore, in most indoor environment, there are many WLAN transmitters that can be used in localization without additional cost, since most computers today are capable of this wireless communication.

There have been researches on RSSI-based localization in logistic applications to track products, assets or equipment. For example, in [11], the RSSI is used in multilateration scheme in wireless sensor network in food transportation. Also, the paper [12] proposes the localization scheme based on spatial reasoning filter using several sensor nodes in various directions, by moving sensor nodes, which is opposing to temporal filter that acquires multiple RSSI at the same location. Similar application can be found from the paper [13] that studies and testes various localization method to track the material in construction site.

The recent work on RSSI/IMU-based localization can be found in [14], where it applies the particle filter as a localization algorithm to track a pedestrian with foot-mounted IMUs and uses RSSI from WiFi access points to compensate the drift error from an IMU. The paper also uses the precise model of the map to constraint or narrow down the possibility of the pedestrian location. Another key important idea is that the way to detect when the pedestrian stop walking and then velocity is reset in both longitudinal and lateral directions to reduce drift error.

The RSSI-based localization that uses the robust extended Kalman filter (EKF) can be found in [15], [16]. The former paper deals with the tracking of cellular phone user in the service cells to improve quality of service. The results are presented by simulation. The later paper proposes the localization method to locate the mobile robot in indoor environment. The experimental results are based on dedicated wireless communication links that can measure the receiving analog power signal directly, which is opposing to our system that obtains the RSSI information with low sampling rate and high quantization noise.

In this work, we study the possibility of using sensor fusion from a low cost IMU and RSSIs by using the EKF for mobile unit localization in two-dimensional plane. The information from an IMU, which is velocity in this study, suffers a tiny bias causing drift error in long run. On the other hand, the information of an RSSI, based on IEEE802.11b standard, is corrupted by large multi-path fading effect and quantization noise. Also, the RSSI information is available in lower sampling rate than of the IMU. The test bed is performed in indoor environment by moving the mobile platform in the predefined path repeatedly to verify the accuracy of algorithm.

The sampling rate of the RSSI data is 4 times slower than of the IMU. Hence, we also study multi-rate sampling setting. That is, we first reduce the sampling rate of the IMU down to match with the one from RSSI. Then, we increase the sampling rate of IMU and use zero-order hold to up sample the RSSI information to match the IMU rate.

Furthermore, we also study the possibility of using smallest number of reference nodes for RSSI. Firstly, we use RSSI information from four reference nodes to fuse with the IMU information. This, in fact, is redundant. Then we reduce the numbers of reference node to validate the possibility and performance.

The body of the paper is organized as follows. In section 2, we address the problem by using simple kinematic model of moving object and discuss the

characteristic of the measurement equations from both sensors. In section 3, we briefly present the well-known EKF algorithm. The experimental results will be presented in section 4, and the conclusions are drawn in section 5 to sum up our work.

2 SYSTEM MODELING

2.1 Kinematic Model

To simplify the sensor fusion scheme, the kinematic model of the vehicle, i.e., position and velocity will be used. Now, let p^x, p^y, v^x, v^y denote position and velocity in x and y direction in Cartesian space respectively. Then, let $x = \begin{bmatrix} p^x & p^y & v^x & v^y \end{bmatrix}^T$. In this note, we consider the control signal as unknown command or acceleration denoted by u. Note that, the acceleration in current velocity direction could be regarded as uncertainty to the system model. Now consider the kinematic model of the vehicle in discrete-time as follows:

$$x(k+1) = Ax(k) + Bu(k), \forall k \in \mathbb{Z}^+, \tag{1}$$

where

$$A = \begin{bmatrix} 1 & 0 & T & 0 \\ 0 & 1 & 0 & T \\ 0 & 0 & 1 & 0 \\ 0 & 0 & 0 & 1 \end{bmatrix}, B = \begin{bmatrix} 0 & 0 \\ 0 & 0 \\ T & 0 \\ 0 & T \end{bmatrix},$$

and T is a sampling time. The goal is to estimate the position of above mobile platform from IMU and RSSI sensing systems.

2.2 IMU Measurement Model

The IMU using in this work is low-cost microcomputer embedded system, around US$100, composing of three-axis accelerometers, rate gyro and magnetic compass sensor that provides many outputs including the raw data from accelerometers, gyroscopes and magnetometer, as well as processed output including linear velocity and attitude. In our study, however, we consider only the velocity output. Hence from above state space representation, we can describe measurement equation from the IMU as follow:

$$y_k^i = \begin{bmatrix} 0 & 0 & -\sin\theta & \cos\theta \\ 0 & 0 & \cos\theta & \sin\theta \end{bmatrix} x_k + \begin{bmatrix} 1 & 0 \\ 0 & 1 \end{bmatrix} \begin{bmatrix} b^x \\ b^y \end{bmatrix} + v_k^i, \tag{2}$$

where θ is an alignment angle between any reference frame and IMU frame referencing to the magnetic north pole with positive angle measuring in clockwise (see Fig. ***1***) direction, b^x and b^y are bias noises, and v^i is a general measurement noise.

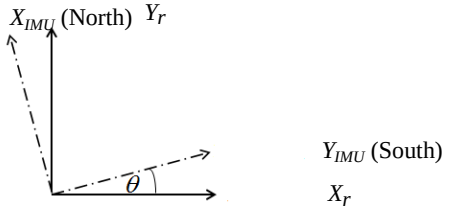

Fig. 1 *Reference frame versus IMU frame.*

Since the bias noises have significant impact, so it is common in localization scheme that this bias noises are modeled as constants or slowly change values, and hence can be incorporated in system modeling. That is, let new state variable

$$x := \begin{bmatrix} p^x & p^y & v^x & v^y & b^x & b^y \end{bmatrix}^T.$$

Hence, we can modify the state space description as follow:

$$x_{k+1} = Ax_k + Bu_k + w_k, \forall k \in \mathbb{Z}^+, \tag{3}$$

where w_k could be considered as uncertainties or disturbances to the system, disturbing the bias state in particular, and

$$A=\begin{bmatrix}1&0&T&0&0&0\\0&1&0&T&0&0\\0&0&1&0&0&0\\0&0&0&1&0&0\\0&0&0&0&1&0\\0&0&0&0&0&1\end{bmatrix},\ B=\begin{bmatrix}0&0\\0&0\\T&0\\0&T\\0&0\\0&0\end{bmatrix}.$$

Therefore, the new measurement from the IMU can be rewritten as

$$y_k^i=\begin{bmatrix}0&0&-\sin\theta&\cos\theta&0&0\\0&0&\cos\theta&\sin\theta&0&0\end{bmatrix}x_k+v_k^i. \quad (4)$$

From our experiment, it is obvious that even a tiny bias in IMU, as in Fig. 2, makes a significant drift in position as depicted in Fig. 3. Note that, Fig. 3 is the result of the Kalman filter that is solely based on the IMU data.

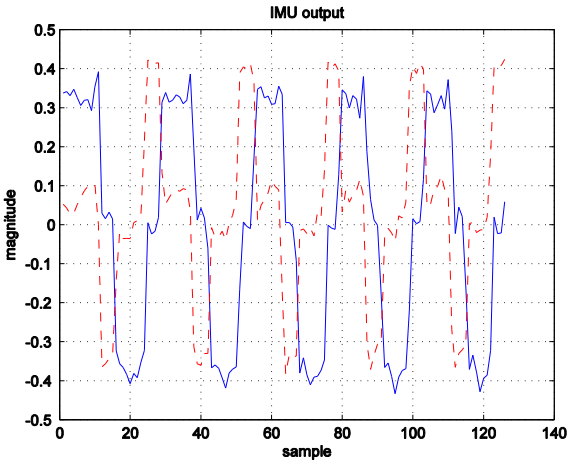

Fig. 2 *Output (velocity) from IMU in both directions.*

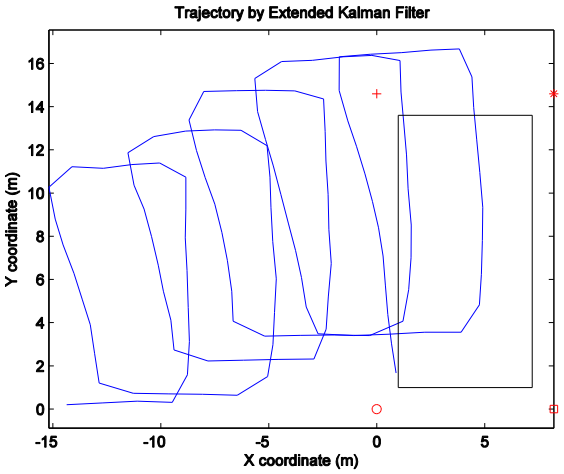

Fig. 3 *Reconstructed map from IMU output only.*

2.3 RSSI Measurement Model

It is well known in the radio communication that transmitted power loss, known as path loss, at the receiver side is related to distance between them. The relation between RSSI and distance is described by ([17], [18])

$$P_r=P_0-10\gamma\log_{10}(d)+v_k^r, \quad (5)$$

where P_r is the power at the receiver side in dB, P_0 is a constant depending on transmitted power, antenna characteristic and average channel attenuation, γ is a path loss exponent, and P_k^r is a measurement noise dominated by shadowing fading [17], [15]. In above equation, two major factors, that make it very difficult to derive distance d, are the path loss exponent and shadowing fading. The path loss exponent γ depends on environment; for example, $\gamma=2$ in the open space and it may be in the range of 1.6-3.5 in an office; see, for example, Table 2 in [17] or Table 4.2 in [19]. The shadowing fading or multipath fading causes unexpected high power at the receiver that averages them from multiple received data packets. The example of the RSSI measured versus distance is shown in Fig. 4, in which large variation is obviously observed. Also, in Fig. 6, the measured RSSI during the experiment comparing with the ideal one computed by using reference moving path shows significant effect of

shadowing fading that causing abnormally high RSSI. The reconstructed map from the EKF based only on RSSI from four reference nodes is shown in Fig. 5. Comparing with the result from IMU in Fig. 3, the result from RSSI only has no drift, but it is not in the good shape of reference path.

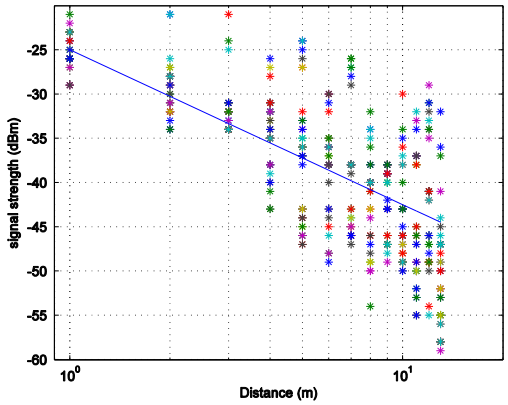

Fig. 4 *Example of RSSI versus distances, solid line is the approximate model.*

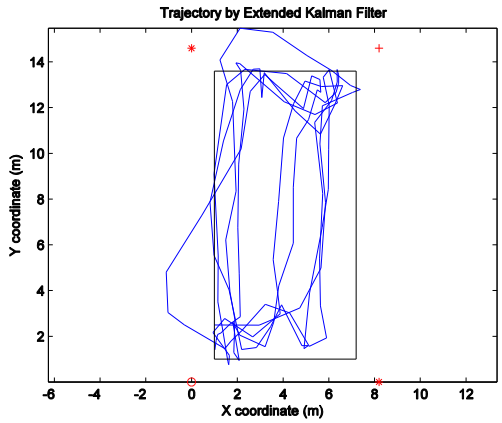

Fig. 5 *Reconstructed map from RSSI output only.*

Now the equation (5) can be used to characterize our measurement equations with multiple references. Let (p_i^x, p_i^y) denote the position of the ith reference. Then we can define the measurement equations from RSSI, for $i = 1,2,\ldots$, related to our system as

$$y_k^{ri} = P_0^i - 10\gamma \log_{10}\left(d^i\right) + v_k^{ri}, \tag{5}$$

where $d^i = \sqrt{\left(p^x - p_i^x\right)^2 + \left(p^y - p_i^y\right)^2}$. In our experiment, we have four access points as the reference nodes.

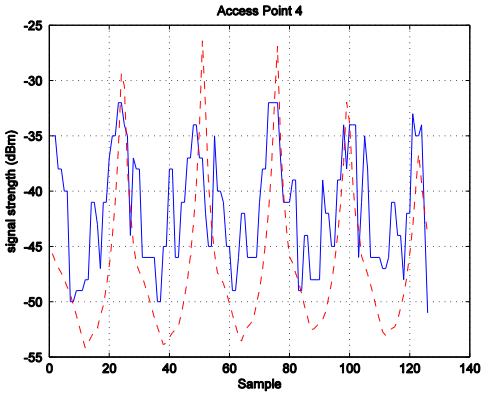

Fig. 6 *RSSI from one of reference access point during experiment (solid line) comparing to ideal one (dash line) inheriting from known reference moving path.*

3. EXTENDED KALMAN FILTER

Since the EKF is well known (e.g., see [20], [21]), and widely used as a linearized version of the Kalman filter for nonlinear system, we, therefore, briefly give some details of it. Consider a general nonlinear system:

$$\begin{aligned} x_{k+1} &= \mathcal{F}_k(x_k, u_k, k) + w_k; \\ y_k &= \mathcal{H}_k(x_k, k) + \upsilon_k, \end{aligned} \tag{6}$$

where w_k and υ_k are process and measurement noises respectively. These noises are assumed to be white Gaussian noise with known covariance as $\mathrm{E}\left[w_k \cdot w_k^T\right] = Q$ and $\mathrm{E}\left[\upsilon_k \cdot \upsilon_k^T\right] = R$, where $\mathrm{E}[\cdot]$ denotes the mathematic expectation. In our case, w_k could be considered as the uncertainty from inaccurate modeling. In practice, these noise covariance serve as tuning parameters of the filter, and could be adjusted based on the empirical experiment. Also, since the existence of the solution of the EKF is not guaranteed to exist for all time, Q and R weighting matrices also serve as tuning parameters for stability of the filter. In addition, we assume that $\mathrm{E}\left[x_0\right] = \eta$ and

$\mathrm{E}\left[(x_0-\eta)\cdot(x_0-\eta)^T\right]=\Xi$ Then, the EKF could be summed up as follows:

$$\begin{aligned}
\hat{x}_{k+1}^- &= \mathcal{F}_k(\hat{x}_k, u_k, k);\\
\hat{y}_{k+1} &= \mathcal{H}_{k+1}(\hat{x}_{k+1}^-);\\
\hat{x}_{k+1} &= \hat{x}_{k+1}^- + K_{k+1}(y_{k+1}-\hat{y}_{k+1});\\
P_{k+1}^- &= F_k P_k F_k^T + Q_k;\\
K_{k+1} &= P_{k+1}^- H_{k+1}^T\left(H_{k+1}P_{k+1}^- H_{k+1}^T + R_{k+1}\right)^{-1};\\
P_{k+1} &= \left(I - K_{k+1}H_{k+1}\right)P_{k+1}^-,
\end{aligned} \tag{7}$$

with initial conditions $\hat{x}_0=\eta$, and $P_0=\Xi$, and where F_k and H_k are the Jacobian matrices, i.e.,

$$F_k=\left.\frac{\partial\mathcal{F}}{\partial x}\right|_{x=\hat{x}_k^-}, H_k=\left.\frac{\partial\mathcal{H}}{\partial x}\right|_{x=\hat{x}_k^-}.$$

4. EXPERIMENTAL RESULTS

In our experiment, we manually move the wheel mobile platform equipped with the IMU sensor, the WLAN receiver that communicates to four access points, and reports all the RSSIs. The IMU, as shown in Fig. 7, used in this experiment is aMG IMU-9A having three-axis accelerometers chip set LSM303DLH, three-axis gyroscope chip set L3G4200D and a magnetometer chip set LSM303DLH. The velocity is computed by microcontroller from the IMU raw data with equations suggested in the product manual. The wireless communication is the IEEE802.11b standard with 2.4GHz carrier frequency with access point model Aolynk WAP500ag as shown in Fig. 8.

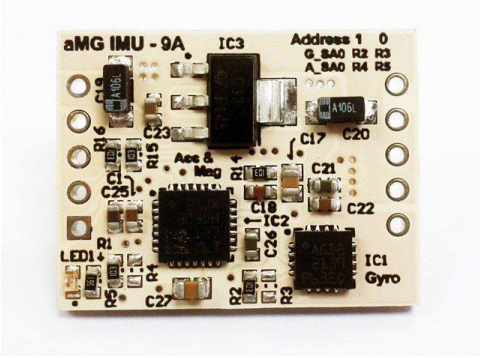

Fig. 7 *IMU sensor module used in the experiment.*

Fig. 8 *IEEE802.11b wireless access point.*

The experiment is conducted by moving the mobile platform in predefine rectangular path for five rounds. The RSSI information is sampled every 4 seconds, while the IMU information is sampled every 1 second.

4.1 Effect of sampling time

Since the sampling rate of the RSSI information is much slower than of the IMU, so we study the effect of using different sampling rate inside the fusion algorithm. We compare three different use of sampling time; that is 4 seconds, 2 seconds, and 1 second. Simple zero order hold is used for up sampling. That is, for $T=4$, the information from the IMU is down sampled by 4, for $T=2$, the information from the IMU is down sampled by 2 when the information from RSSI is up sampled by 2, and for $T=1$, the information from the RSSI is up sampled by 4.

The EKF in (7) is performed, where dynamics $\mathcal{F}_k$ equals to (3), and measurement equation $\mathcal{H}_k$ is from (4) and (5); that is

$$\mathcal{H}_k=\begin{bmatrix}
-\hat{x}_3\sin\theta+\hat{x}_4\cos\theta+\hat{x}_5\\
\hat{x}_3\cos\theta+\hat{x}_4\sin\theta+\hat{x}_6\\
-24-25\log_{10}\left(\sqrt{\hat{x}_1^2+\hat{x}_2^2}\right)\\
-33-25\log_{10}\left(\sqrt{\hat{x}_1^2+(\hat{x}_2-14.6)^2}\right)\\
-33-25\log_{10}\left(\sqrt{(\hat{x}_1-8.2)^2+(\hat{x}_2-14.6)^2}\right)\\
-24-25\log_{10}\left(\sqrt{(\hat{x}_1-8.2)^2+\hat{x}_2^2}\right)
\end{bmatrix},$$

where

$\theta=0.1$ rad. The EKF parameters are of follows: $\hat{x}_0=\begin{bmatrix}1 & 1 & 0 & 0.1 & 0 & 0\end{bmatrix}^T$ and $P_0=10^{-6}I_{6\times6}$.

For different sampling time, we use different weighting matrices of process and measurement noise covariance as shown in Table 1 below.

Table 1 *Noise covariance in different sampling time*

T	Q, R
4	$Q = 10^{-3}\,\mathrm{diag}(1,1,0.1,0.1,10^{-6},10^{-6})$ $R = \mathrm{diag}(40,40,40,40,10^{-4},10^{-4})$
2	$Q = 10^{-3}\,\mathrm{diag}(1,1,0.1,0.1,2\cdot10^{-6},2\cdot10^{-6})$ $R = \mathrm{diag}(7,7,7,7,10^{-4},10^{-4})$
1	$Q = 3\times10^{-4}\,\mathrm{diag}(1,1,0.1,0.1,10^{-5},10^{-5})$ $R = \mathrm{diag}(1,1,1,1,10^{-5},10^{-5})$

The experimental data from the IMU is shown in Fig. 2, and the comparison to the output from the EKF (for $T = 4$ sec.) is shown in Fig. 9. It can be seen from the Fig. 9 that the estimated velocity from the EKF shows less significant bias in comparison with the velocity output from the IMU, particularly in y-direction. Also, the comparisons of the actual RSSIs from four access points and the estimate from the EKF are depicted in Fig. 10. It is obvious that the estimated RSSI is significantly smoother than the sensor one, and corresponds to the moving pattern which is high power when the platform moves close to the access point and low power when it moves away. The bias states in both directions are shown in

Fig. ***11***.

The estimate position in x-y coordinate from the EKF is plotted together with the reference moving path in Fig. 12 to Fig. 14 for $T = \{4,2,1\}$ respectively. It is obvious that the position outputs from the EKF in three cases are close to the reference path with no drift effect; see Fig. 3 and Fig. 5. for comparison.

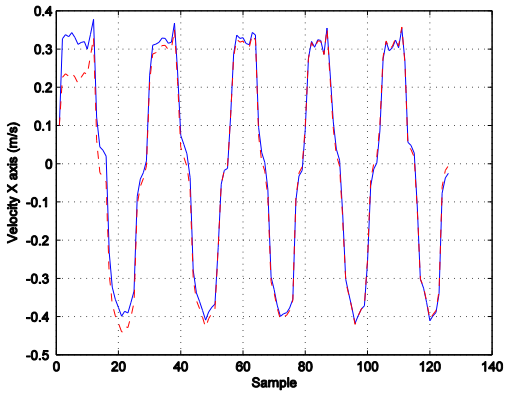

(a) x-direction

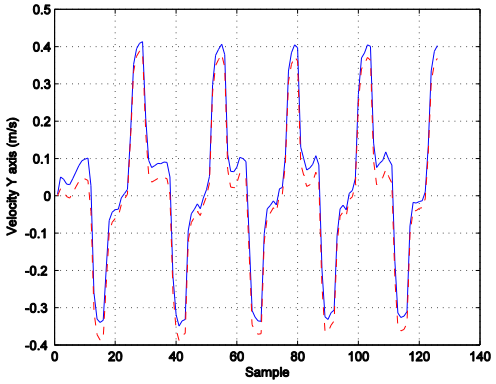

(b) y-direction

Fig. 9 *Estimated and actual IMU output comparison: solid line and dash line are actual and estimate IMU output respectively.*

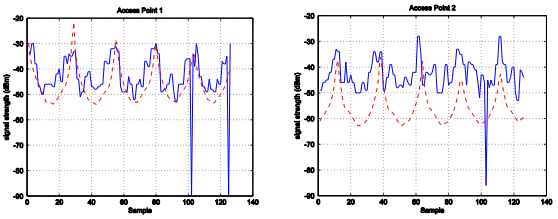

(a) access point no. 1 (b) access point no. 2

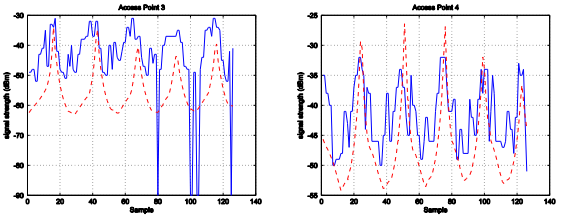

(c) access point no. 3 (d) access point no. 4

Fig. 10 *Estimated and actual RSSI output comparison: solid line and dash line are actual and estimate RSSI output respectively.*

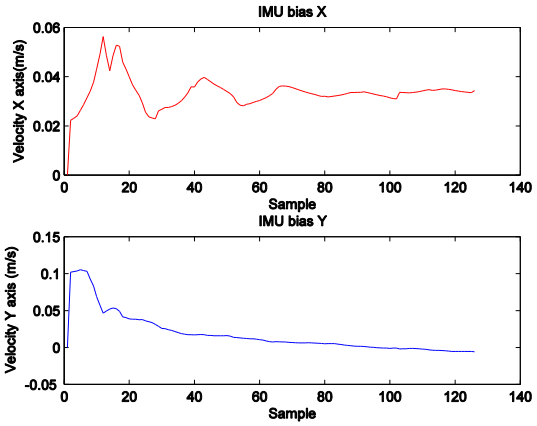

Fig. 11 *IMU bias state in both x and y directions from the EKF when* $T = 4$.

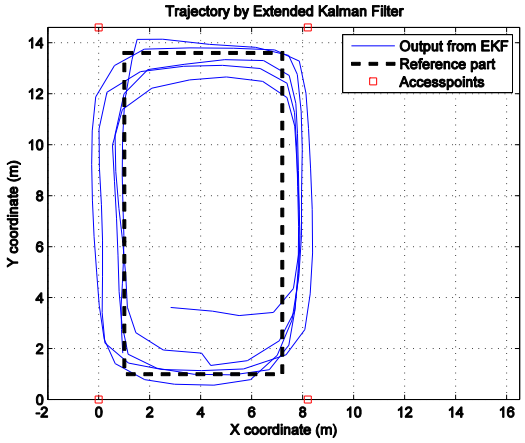

Fig. 12 *Reconstructed map from the EKF when* $T = 4$.

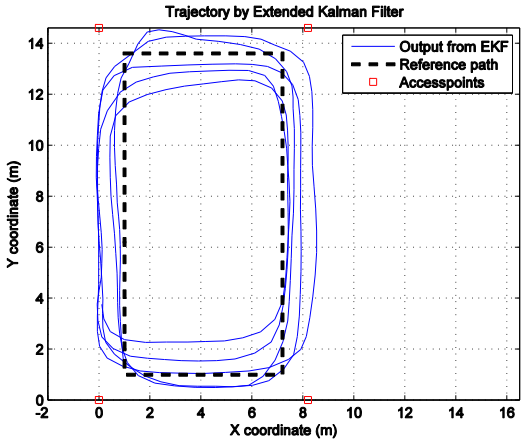

Fig. 13 *Reconstructed map from the EKF when* $T = 2$

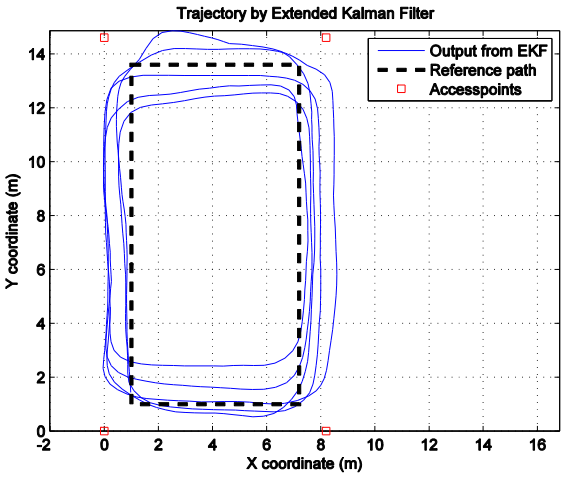

Fig. 14 *Reconstructed map from the EKF when* $T = 1$.

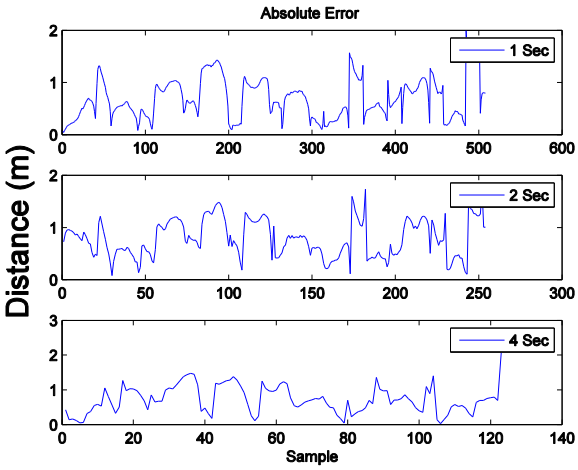

Fig. 15 *Comparison of absolute error for different sampling time.*

The comparison of root mean square (RMS) error in each case is shown in Table 2 below. Also the comparison of the absolute error and the trace of error covariance are shown in

Fig. *15* and Fig. 16. Note that, the covariance matrix P_k is normally used to indicate the convergent of the filter, and, hence, it is useful in the tuning process. Note that even the shorter sampling time yield lower RMS error, but the difference is not significant. So the EKF, in this experiment, is robust to sampling period. In fact, it depends on the dynamics of the moving platform.

Table 2 *Comparison of RMS error for different sampling time*

T (sec)	RMS error (meter)
4	0.8832
2	0.8661
1	0.7860

4.1 Effect of number of nodes

Although, in theory, three reference nodes are sufficient to uniquely determine the position of a mobile unit, in practice, however, more reference nodes will provide better result. In previous setup, we validate the possibility of the fusion scheme in well setup environment having 4 reference nodes for RSSI. In this subsection, we study the possibility of using smallest number of reference nodes, since the information from the RSSI can be considered as an assistance to the IMU.

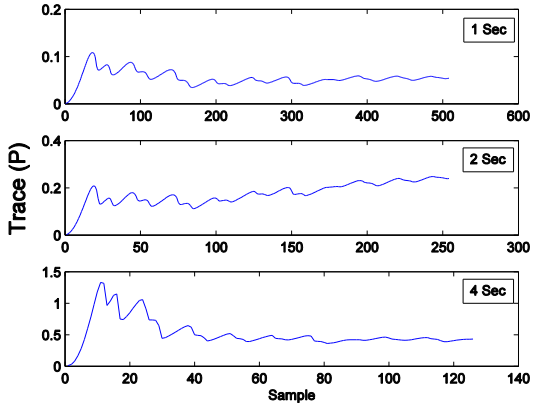

Fig. 16 *Comparison of trace of error covariance (*$\text{trace}\left(P_k\right)$*) for different sampling time.*

Thus, from previous raw information from both RSSI and IMU, we reduce the number of the RSSI information from 4 nodes to 3, 2 and 1. The base line is the result from previous subsection having 4 reference nodes and sampling time $T = 1\,\text{sec}$. Different value for noise covariance weighting matrices are used in different numbers of reference nodes as shown in Table 3 below.

Table 3 *Noise covariance in different number of reference node (#N).*

#N	Q, R
3	$Q = 2\cdot 10^{-3}\,\text{diag}(1,1,0.1,0.1,2\cdot 10^{-6},2\cdot 10^{-6})$ $R = 10^{2}\,\text{diag}(5,5,5,10^{-6},10^{-6})$
2	$Q = 9\cdot 10^{-3}\,\text{diag}(1,1,0.1,0.1,2\cdot 10^{-7},2\cdot 10^{-7})$ $R = \text{diag}(800,800,10^{-3},10^{-3})$
1	$Q = 10^{-2}\,\text{diag}(1,1,0.1,0.1,2\cdot 10^{-8},2\cdot 10^{-8})$ $R = \text{diag}(7\cdot 10^{3},10^{-2},10^{-2})$

The resulting maps from fusion algorithm with 3 different numbers of reference nodes are depicted in Fig. 17 - Fig. 19, and the comparison of RMS error is shown in Table 4. Also the comparison of the absolute error and the trace of error covariance are shown in Fig. 20 and Fig. 21. From those results, it is obvious that using more reference nodes provides better results. However, with reduced number of reference nodes, the reconstruct map from the EKF still yields the shape of reference path, but, of course, with higher error. It is worth noting that the fusion from IMU has contribution to this situation when multiple reference nodes are not available.

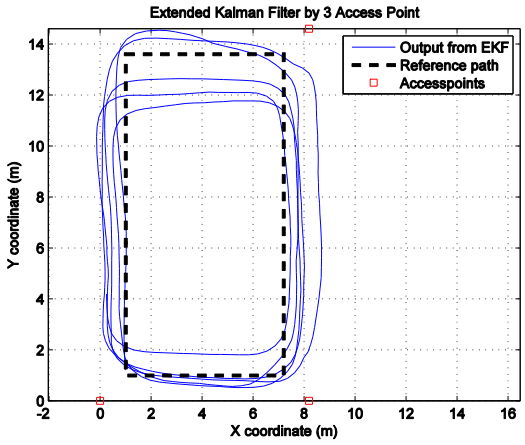

Fig. 17 *Reconstructed map from the EKF with 3 reference nodes.*

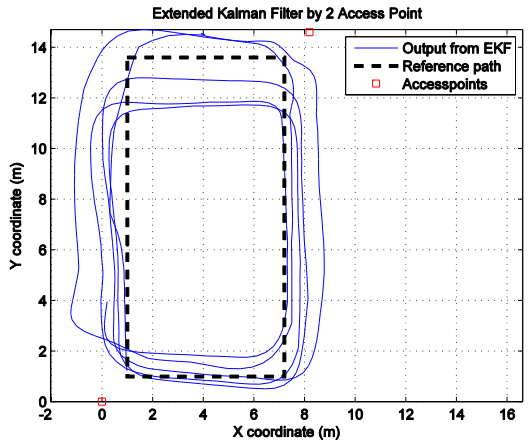

Fig. 18 *Reconstructed map from the EKF with 2 reference nodes.*

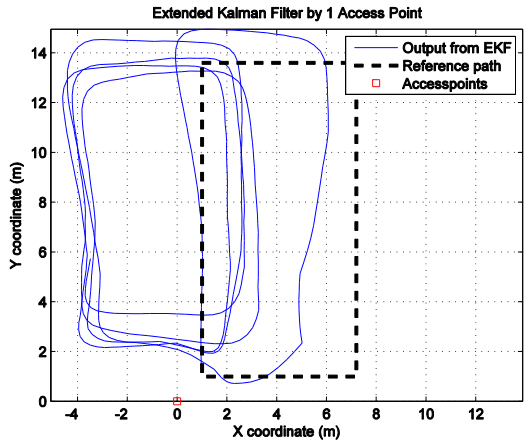

Fig. 19 *Reconstructed map from the EKF with 1 reference nodes.*

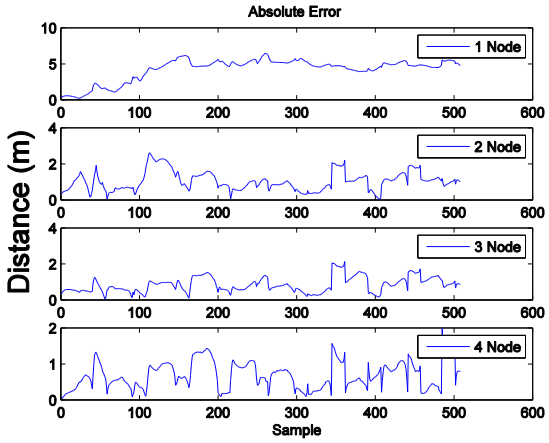

Fig. 20 *Comparison of absolute error for different number of reference node.*

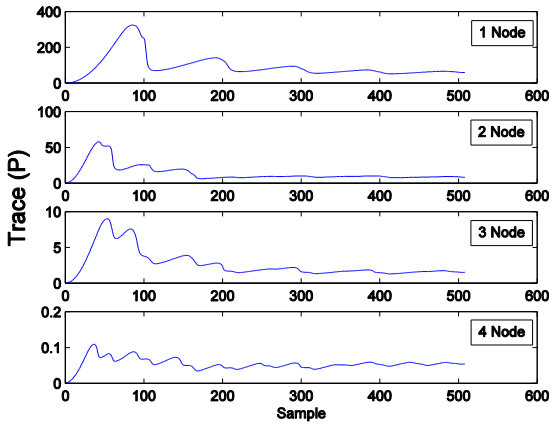

Fig. 21 *Comparison of trace of error covariance (*$\text{trace}\left(P_k\right)$*) for different number of reference node.*

Table 4 *RMS error versus different number of reference node (#N).*

#N	RMS error (meter)
4	0.7860
3	0.9389
2	1.1643
1	4.4971

5. CONCLUSION

This paper proposes the fusion algorithm by using RSSI/IMU sensor for localization problem of a mobile unit in indoor environment where GPS is invalid. The information from both sensors corrupted by noise and uncertainties are fused by the EKF. The results show that this IMU/RSSI sensor fusion is a promising for indoor environment that can handle the bias problem from the IMU, and is robust to various uncertainties from the RSSI measurement. The best result, obviously, based on fastest sampling time and four referent nodes achieving sub meter level of RMS error.

Further studies on sampling time, also show that this sensor fusion scheme is robust to various value of sampling period. This advantage is significant in practice when the acquisition of the RSSI is much slower than the IMU so that the single sampling rate can be applied. High sampling frequency obviously provides good result especially at the turning corners, since the

mobile unit change velocity abruptly, and the fast accessing to IMU can capture that movement. It is also worth noting that with simple zero order hold for RSSI information, we can increase sampling rate to match the IMU sampling rate without the need of multi-rate scheme and still yields good results.

We also further study on reducing the numbers of reference nodes, and the results show that it can achieve down to two reference nodes with promising results. This is very significant in practice when the mobile unit may loss communication to reference nodes from time to time. For one reference nodes, however, it seems that it cannot compensate the drift of the IMU.

The EKF, however, needs some parameter tuning especially process and measurement noise covariance Q, R. For the future work, we will work on the method to calibrate some parameters in measurement, such as P_0, γ autonomously. Also, the fusion algorithm could be improved by some adaptive schemes for adjusting the process and measurement noise covariance, or applying other estimation methods such as unscented Kalman filter.

REFERENCES

[1] J. Borenstein, H. Everett, L. Feng, and D. Wehe, "Mobile robot positioning-sensors and techniques," DTIC Document, Tech. Rep., 1997.

[2] G. Dudek and M. Jenkin, *Computational principles of mobile robotics*. Cambridge university press, 2010.

[3] F. Caron, E. Duflos, D. Pomorski, and P. Vanheeghe, "GPS/IMU data fusion using multisensor kalman filtering: introduction of contextual aspects," *Information Fusion*, vol. 7, no. 2, pp. 221 – 230, 2006. [Online]. Available: http://www.sciencedirect.com/-science/article/pii/S156625350400065X

[4] A. Brown, "GPS/INS uses low-cost MEMS IMU," *Aerospace and Electronic Systems Magazine, IEEE*, vol. 20, no. 9, pp. 3–10, 2005.

[5] E. Shin and N. El-Sheimy, *Accuracy improvement of low cost INS/GPS for land applications*. University of Calgary, Department of Geomatics Engineering, 2001.

[6] A. H. Mohamed and K. P. Schwarz, "Adaptive Kalman Filtering for INS/GPS," *Journal of Geodesy*, vol. 73, pp. 193–203, 1999. [Online]. Available: http://dx.doi.org/10.1007/s001900050236

[7] J. Corrales, F. Candelas, and F. Torres, "Hybrid tracking of human operators using IMU/UWB data fusion by a Kalman filter," in *Human-Robot Interaction (HRI), 2008 3rd ACM/IEEE International Conference on*, march 2008, pp. 193 –200.

[8] G. Scandaroli and P. Morin, "Nonlinear filter design for pose and IMU bias estimation," in *Robotics and Automation (ICRA), 2011 IEEE International Conference on*, may 2011, pp. 4524 –4530.

[9] G. Scandaroli, P. Morin, and G. Silveira, "A nonlinear observer approach for concurrent estimation of pose, IMU bias and camera-to-IMU rotation," in *Intelligent Robots and Systems (IROS), 2011 IEEE/RSJ International Conference on*, sept. 2011, pp. 3335 – 3341.

[10] B. Khaleghi, A. Khamis, F. O. Karray, and S. N. Razavi, "Multisensor data fusion: A review of the state-of-the-art," *Information Fusion*, vol. 14, no. 1, pp. 28 – 44, 2013. [Online]. Available: http://www.sciencedirect.com/science/article/pii/-S1566253511000558

[11] X. Wang, O. Bischoff, R. Laur, and S. Paul, "Localization in Wireless Ad-hoc Sensor Networks using Multilateration with RSSI for Logistic Applications," *Procedia Chemistry*, vol. 1, no. 1, pp. 461 – 464, 2009, <ce:title>Proceedings of the Eurosensors XXIII conference</ce:title>. [Online]. Available: http://www.sciencedirect.com/science/article/pii/-S1876619609001168

[12] X. Wang, S. Yuan, R. Laur, and W. Lang, "Dynamic localization based on spatial reasoning with RSSI in wireless sensor networks for transport logistics," *Sensors and Actuators A: Physical*, vol. 171, no. 2, pp. 421 – 428, 2011. [Online]. Available: http://-www.sciencedirect.com/science/article/pii/S092442471100495X

[13] X. Luo, W. J. O'Brien, and C. L. Julien, "Comparative evaluation of Received Signal-Strength Index (RSSI) based indoor localization techniques for construction jobsites," *Advanced Engineering Informatics*, vol. 25, no. 2, pp. 355 – 363, 2011. [Online]. Available: http://www.sciencedirect.com/science/-article/pii/S1474034610000984

[14] O. Woodman and R. Harle, "Pedestrian localisation for indoor environments," in *Proceedings of the 10th international conference on Ubiquitous computing*, ser. UbiComp '08. New York, NY, USA: ACM, 2008, pp. 114–123. [Online]. Available: http://doi.acm.org/10.1145/1409635.1409651

[15] P. N. Pathirana, A. V. Savkin, and S. Jha, "Robust extended Kalman filter based technique for location management in PCS networks," *Computer Communications*, vol. 27, no. 5, pp. 502 – 512, 2004. [Online]. Available: http://www.sciencedirect.com/-science/article/pii/S0140366403002871

[16] P. N. Pathirana, N. Bulusu, A. V. Savkin, and S. Jha, "Node localization using mobile robots in delay-tolerant sensor networks," *Mobile Computing, IEEE Transactions on*, vol. 4, no. 3, pp. 285 – 296, may-june 2005.

[17] Z. Ren, G. Wang, Q. Chen, and H. Li, "Modelling and simulation of Rayleigh fading, path loss, and shadowing fading for wireless mobile networks," *Simulation Modelling Practice and Theory*, vol. 19, no. 2, pp. 626 – 637, 2011. [Online]. Available: http://-www.sciencedirect.com/science/article/pii/S1569190X10002017

[18] F. Vanheel, J. Verhaevert, E. Laermans, I. Moerman, and P. Demeester, "Automated linear regression tools improve RSSI WSN localization in multipath indoor environment," *EURASIP Journal on Wireless Communications and Networking*, vol. 2011, pp. 1–27, 2011. [Online]. Available: http://dx.doi.org/10.1186/-1687-1499-2011-38

[19] T. S. Rappaport, *Wireless Communications: Principles and Practice*, 1st ed. Piscataway, NJ, USA: IEEE Press, 1996.

[20] B. D. O. Anderson and J. B. Moore, *Optimal Filtering*. Englewood Cliffs, N.J.: Prentice Hall, 1979.

[21] I. R. Petersen and A. V. Savkin, *Robust Kalman Filtering for Signals and Systems with Large Uncertainties*. Boston: Birkhäuser, 1999.

Warapon Kumkaew received her Bachelor degree in Machatronics Engineering from Mahanakorn University of Technology in 2010. She is currently studying the Master degree program in Control Engineering at Mahanakorn University of Technology.

Veerachai Malyavej received his B.Eng in electronics engineering from King Mongkut's Institute of Technology Ladkrabang, Bangkok, Thailand in 1996, M.EngSc. and PhD., in electrical engineering (systems and control) from the University of New South Wale, Sydney, Australia in 2002 and 2006 respectively. He has been with the Department of Control, Instrumentation and Mechatronics Engineering, Mahanakorn University of Technology since 1996. His research interest includes optimal and robust control, state estimation and filtering, robotic particularly in localization and guidance.

Manop Aorpimai received his Bachelor of Engineering (Control Engineering) degree from the King Mongkut's Institute of Technology, Ladkrabang, Bangkok in 1994, and completed his Ph.D. degree in Satellite Engineering from the Surrey Space Centre, University of Surrey, United Kingdom in 2000. Currently, he is a lecturer at the Department of Control and Instrumentation Engineering, Mahanakorn University of Technology, Thailand. His research interests include vehicle localization, spacecraft orbit and attitude determination and control, modern control theory and applications.